

Measurement of Heavy Gauge Bosons in Little Higgs Model with T-parity at ILC

Yosuke Takubo¹, Eri Asakawa², Masaki Asano¹, Keisuke Fujii³, Tomonori Kusano¹, Shigeki Matsumoto⁴, Rei Sasaki¹, and Hitoshi Yamamoto¹

1- Department of Physics, Tohoku University, Sendai, Japan

2- Institute of Physics, Meiji Gakuin University, Yokohama, Japan

3- High Energy Accelerator Research Organization (KEK), Tsukuba, Japan

4- Department of Physics, University of Toyama, Toyama, Japan

The Littlest Higgs Model with T-parity is one of the attractive candidates of physics beyond the Standard Model. One of the important predictions of the model is the existence of new heavy gauge bosons, where they acquire mass terms through the breaking of global symmetry necessarily imposed on the model. The determination of the masses are, hence, quite important to test the model. In this paper, the measurement accuracy of the heavy gauge bosons at ILC is reported.

1 Introduction

There are a number of scenarios for new physics beyond the Standard Model. The most famous one is the supersymmetric scenario. Recently, alternative one called the Little Higgs scenario has been proposed [1, 2]. In this scenario, the Higgs boson is regarded as a pseudo Nambu-Goldstone boson associated with a global symmetry at some higher scale. A Z_2 symmetry called T-parity is imposed on the models to satisfy constraints from electroweak precision measurements [3, 4, 5]. Under the parity, new particles are assigned to be T-odd (i.e. with a T-parity of -1), while the SM particles are T-even. The lightest T-odd particle is stable and provides a good candidate for dark matter. In this article, we focus on the Littlest Higgs model with T-parity as a simple and typical example of models implementing both the Little Higgs mechanism and T-parity.

In order to test the Little Higgs model, precise determinations of properties of Little Higgs partners are mandatory, because these particles are directly related to the cancellation of quadratically divergent corrections to the Higgs mass term. In particular, measurements of heavy gauge boson masses, Little Higgs partners for gauge bosons, are quite important. Since heavy gauge bosons acquire mass terms through the breaking of the global symmetry, precise measurements of their masses allow us to determine the most important parameter of the model, namely the vacuum expectation value of the breaking.

We studied the measurement accuracy of masses of the heavy gauge bosons at the international linear collider (ILC). In addition, the sensitivity to the vacuum expectation value (f) was estimated. In this paper, the status of the study is shown, and the detail of this study is described in [6].

2 Representative point and target mode

In order to perform a numerical simulation at ILC, we need to choose a representative point in the parameter space of the Littlest Higgs model with T-parity. Firstly, the model parameters should satisfy the current electroweak precision data. In addition, the cosmological

\sqrt{s}	$e^+e^- \rightarrow A_H Z_H$	$e^+e^- \rightarrow Z_H Z_H$	$e^+e^- \rightarrow W_H^+ W_H^-$
500 GeV	1.91 (fb)	—	—
1 TeV	7.42 (fb)	110 (fb)	277 (fb)

Table 1: Cross sections for the production of heavy gauge bosons.

observation of dark matter relics also gives important information. Thus, we consider not only the electroweak precision measurements but also the WMAP observation [7] to choose a point in the parameter space. We have selected a representative point where Higgs mass and f are 134 GeV and 580 GeV, respectively. At the representative point, we have obtained $\Omega_{\text{DM}} h^2$ of 1.05. The masses of the heavy gauge bosons are $(M_{A_H}, M_{W_H}, M_{Z_H}) = (81.9 \text{ GeV}, 368 \text{ GeV}, 369 \text{ GeV})$, where A_H , Z_H , and W_H are the Little Higgs partners of a photon, Z boson, and W boson, respectively. Here, A_H plays the role of dark matter in this model [8, 9]. Since all the heavy gauge bosons are lighter than 500 GeV, it is possible to generate them at ILC.

There are four processes whose final states consist of two heavy gauge bosons: $e^+e^- \rightarrow A_H A_H$, $A_H Z_H$, $Z_H Z_H$, and $W_H^+ W_H^-$. The first process is undetectable, thus not considered in this article. The cross sections of the other processes are shown in Table 1. Since $m_{A_H} + m_{Z_H}$ is less than 500 GeV, $A_H Z_H$ can be produced at the $\sqrt{s} = 500 \text{ GeV}$. At $\sqrt{s} = 1 \text{ TeV}$, we can observe $W_H^+ W_H^-$ with large cross section. We, hence, concentrate on $e^+e^- \rightarrow A_H Z_H$ at $\sqrt{s} = 500 \text{ GeV}$ and $e^+e^- \rightarrow W_H^+ W_H^-$ at $\sqrt{s} = 1 \text{ TeV}$. Feynman diagrams for the signal processes are shown in Fig. 1. Note that Z_H decays into $A_H h$, and W_H^\pm decays into $A_H W^\pm$ with almost 100% branching fractions.

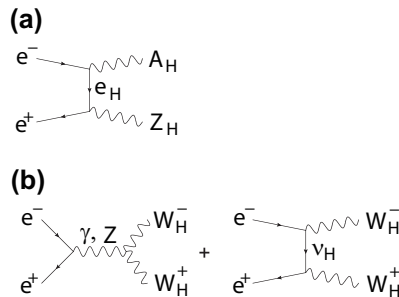


Figure 1: Diagrams for signal processes; (a) $e^+e^- \rightarrow A_H Z_H$ and (b) $e^+e^- \rightarrow W_H^+ W_H^-$.

3 Simulation tools

We have used MadGraph [10] to generate $e^+e^- \rightarrow A_H Z_H$ at $\sqrt{s} = 500 \text{ GeV}$, while $e^+e^- \rightarrow W_H^+ W_H^-$ at $\sqrt{s} = 1 \text{ TeV}$ and all the standard model events have been generated by Physsim [11]. We ignored the initial- and final-state radiation, beamstrahlung, and the beam energy spread for study of $e^+e^- \rightarrow A_H Z_H$ at $\sqrt{s} = 500 \text{ GeV}$, whereas their effects were considered for study of $e^+e^- \rightarrow W_H^+ W_H^-$ at $\sqrt{s} = 1 \text{ TeV}$ where the beam energy spread is set to 0.14% for the electron beam and 0.07% for the positron beam. The finite crossing angle between the electron and positron beams was assumed to be zero. In both event generators, the helicity amplitudes were calculated using the HELAS library [12], which allows us to deal with the effect of gauge boson polarizations properly. Parton showering and hadronization have been carried out by using PYTHIA6.4 [13], where final-state tau leptons are decayed by TAUOLA [14] in order to handle their polarizations correctly. The generated Monte Carlo events have been passed to a detector simulator called JSFQuickSimulator, which implements the GLD geometry and other detector-performance related parameters [15].

Process	Cross sec. [fb]	# of events	# of events after all cuts
$A_H Z_H \rightarrow A_H A_H b\bar{b}$	1.05	525	272
$\nu\nu h \rightarrow \nu\nu b\bar{b}$	34.0	17,000	3,359
$Zh \rightarrow \nu\nu b\bar{b}$	5.57	2,785	1,406
$t\bar{t} \rightarrow WWb\bar{b}$	496	248,000	264
$ZZ \rightarrow \nu\nu b\bar{b}$	25.5	12,750	178
$\nu\nu Z \rightarrow \nu\nu b\bar{b}$	44.3	22,150	167
$\gamma Z \rightarrow \gamma b\bar{b}$	1,200	600,000	45

Table 2: Signal and backgrounds processes considered in the $A_H Z_H$ analysis.

4 Analysis

In this section, we present simulation and analysis results for heavy gauge boson productions. The simulation has been performed at $\sqrt{s} = 500$ GeV for the $A_H Z_H$ production and at $\sqrt{s} = 1$ TeV for the $W_H^+ W_H^-$ production with an integrated luminosity of 500 fb^{-1} .

4.1 $e^+e^- \rightarrow A_H Z_H$ at 500 GeV

A_H and Z_H are produced with the cross section of 1.9 fb at the center of mass energy of 500 GeV. Since Z_H decays into A_H and the Higgs boson, the signature is a single Higgs boson in the final state, mainly 2 jets from $h \rightarrow b\bar{b}$ (with a 55% branching ratio). We, therefore, define $A_H Z_H \rightarrow A_H A_H b\bar{b}$ as our signal event. For background events, contribution from light quarks was not taken into account because such events can be rejected to negligible level after requiring the existence of two b -jets, assuming a b -tagging efficiency of 80% for b -jets with 15% probability to misidentify a c -jet as a b -jet. This b -tagging performance was estimated by the full simulation, assuming a typical ILC detector. Signal and background processes considered in this analysis are summarized in Table 2. Figure 2 shows a typical $A_H Z_H$ event seen in the detector simulator.

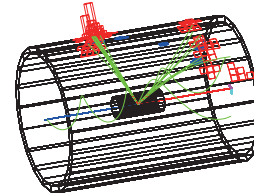


Figure 2: A typical event of $A_H Z_H$ in the simulator.

The clusters in the calorimeters are combined to form a jet if the two clusters satisfy $y_{ij} < y_{\text{cut}}$. y_{ij} is defined as

$$y_{ij} = \frac{2E_i E_j (1 - \cos \theta_{ij})}{E_{\text{vis}}^2}, \quad (1)$$

where θ_{ij} is the angle between momenta of two clusters, $E_{i(j)}$ are their energies, and E_{vis} is the total visible energy. All events are forced to have two jets by adjusting y_{cut} . We have selected events with the reconstructed Higgs mass in a window of 100 – 140 GeV. Since Higgs bosons coming from the WW fusion process have the transverse momentum (p_T) mostly below W mass, p_T is required to be above 80 GeV in order to suppress the $\nu\nu h \rightarrow \nu\nu b\bar{b}$ background. Finally, multiplying the efficiency of double b -tagging ($0.8 \times 0.8 = 0.64$), we are left with 272 signal and 5,419 background events as shown in Table 2, which corresponds

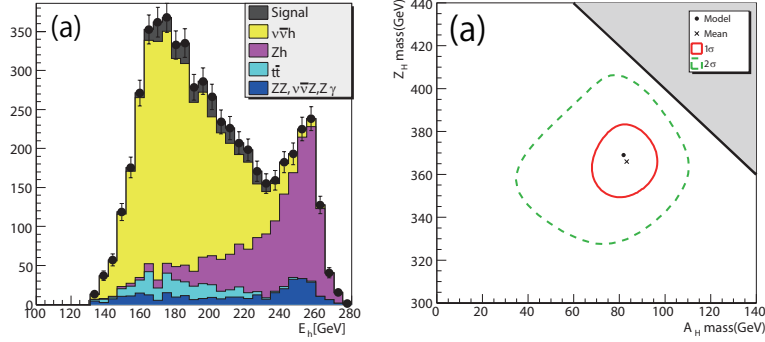


Figure 3: (a) Energy distribution of the reconstructed Higgs bosons with remaining backgrounds after the mass cut. (b) Probability contours corresponding to 1- and 2- σ deviations from the best fit point in the A_H and Z_H mass-plane. The shaded area shows the unphysical region of $m_{A_H} + m_{Z_H} > 500$ GeV.

to a signal significance of 3.7 ($= 272/\sqrt{5419}$) standard deviations. The indication of the new physics signal can hence be obtained at $\sqrt{s} = 500$ GeV.

The masses of A_H and Z_H bosons can be estimated from the edges of the distribution of the reconstructed Higgs boson energies. This is because the maximum and minimum Higgs boson energies (E_{\max} and E_{\min}) are written in terms of these masses,

$$\begin{aligned} E_{\max} &= \gamma_{Z_H} E_h^* + \beta_{Z_H} \gamma_{Z_H} p_h^*, \\ E_{\min} &= \gamma_{Z_H} E_h^* - \beta_{Z_H} \gamma_{Z_H} p_h^*, \end{aligned} \quad (2)$$

where $\beta_{Z_H}(\gamma_{Z_H})$ is the $\beta(\gamma)$ factor of the Z_H boson in the laboratory frame, while $E_h^*(p_h^*)$ is the energy (momentum) of the Higgs boson in the rest frame of the Z_H boson. Note that E_h^* is given as $(M_{Z_H}^2 + M_h^2 - M_{A_H}^2)/(2M_{Z_H})$.

Figure 3(a) shows the energy distribution of the reconstructed Higgs bosons with remaining backgrounds. The background events are subtracted from Fig. 3(a), assuming that the background distribution can be understood completely. Then, the endpoints, E_{\max} and E_{\min} , have been estimated by fitting the distribution with a line shape determined by a high statistics signal sample. The fit resulted in m_{A_H} and m_{Z_H} to be 83.2 ± 13.3 GeV and 366.0 ± 16.0 GeV, respectively, which should be compared to their true values: 81.85 GeV and 368.2 GeV. Figure 3(b) shows the probability contours for the masses of A_H and Z_H .

Since the masses of the heavy gauge bosons are from the vacuum expectation value (f), f can be determined by fitting the energy distribution of the reconstructed Higgs bosons. Then, f was determined to be $f = 576.0 \pm 25.0$ GeV.

4.2 $e^+e^- \rightarrow W_H^+ W_H^-$ at 1 TeV

$W_H^+ W_H^-$ production has large cross section (277 fb) at ILC with $\sqrt{s} = 1$ TeV. Since W_H^\pm decays into A_H and W^\pm with the 100% branching ratio, analysis procedure depends on the W decay modes. In this analysis, we have used 4-jet final states from hadronic decays of

Process	cross sec. [fb]	# of events	# of events after all cuts
$W_{\text{H}}^+ W_{\text{H}}^- \rightarrow A_{\text{H}} A_{\text{H}} qqqq$	106.5	53,258	37,560
$W^+ W^- \rightarrow qqqq$	1773.5	886,770	306
$e^+ e^- W^+ W^- \rightarrow e^+ e^- qqqq$	464.9	232,442	23
$e\nu_e W Z \rightarrow e\nu_e qqqq$	25.5	12,770	3,696
$Z_{\text{H}} Z_{\text{H}} \rightarrow A_{\text{H}} A_{\text{H}} hh$	99.5	49,757	3,351
$\nu\bar{\nu} W^+ W^- \rightarrow \nu\bar{\nu} qqqq$	6.5	3,227	1,486

Table 3: Signal and background processes considered in the $W_{\text{H}}^+ W_{\text{H}}^-$ analysis.

two W bosons, $W_{\text{H}}^+ W_{\text{H}}^- \rightarrow A_{\text{H}} A_{\text{H}} qqqq$. Signal and background processes considered in the analysis are summarized in Table 3.

All events have been reconstructed as 4-jet events by adjusting the cut on y -values. In order to identify the two W bosons from W_{H}^{\pm} decays, two jet-pairs have been selected so as to minimize a χ^2 function,

$$\chi^2 = (\text{rec}M_{W1} - \text{tr}M_W)^2 / \sigma_{M_W}^2 + (\text{rec}M_{W2} - \text{tr}M_W)^2 / \sigma_{M_W}^2, \quad (3)$$

where $\text{rec}M_{W1(2)}$ is the invariant mass of the first (second) 2-jet system paired as a W candidate, $\text{tr}M_W$ is the true W mass (80.4 GeV), and σ_{M_W} is the resolution for the W mass (4 GeV). We required $\chi^2 < 26$ to obtain well-reconstructed events. Since A_{H} bosons escape from detection resulting in a missing momentum, the missing transverse momentum ($^{\text{miss}}p_{\text{T}}$) of the signal peaks at around 175 GeV. We have thus selected events with $^{\text{miss}}p_{\text{T}}$ above 84 GeV. Then, the reconstructed W energy is required to be between 0 GeV to 500 GeV. The numbers of events after the selection cuts are shown in Table 3. The number of remaining background events is much smaller than that of the signal.

As in the case of the $A_{\text{H}} Z_{\text{H}}$ production, the masses of A_{H} and W_{H} bosons can be determined from the edges of the W energy distribution. Figure 4(a) shows the energy distribution of the reconstructed W bosons. After subtracting the backgrounds from Fig.4(a), the distribution has been fitted with a line shape function. The fitted masses of A_{H} and W_{H} bosons are 82.29 ± 1.10 GeV and 367.8 ± 0.8 GeV, respectively, which are to be compared to their input values: 81.85 GeV and 368.2 GeV. Figure 4(b) shows the probability contours for the masses of A_{H} and W_{H} at 1 TeV. The mass resolution improves dramatically at $\sqrt{s} = 1$ TeV, compared to that at $\sqrt{s} = 500$ GeV. Then, $f = 579.7 \pm 1.1$ GeV was obtained by fitting the energy distribution of the reconstructed W bosons.

5 Summary

The Littlest Higgs Model with T-parity is one of the attractive candidates of physics beyond the Standard Model since it solves both the little hierarchy and dark matter problems simultaneously. One of the important predictions of the model is the existence of new heavy gauge bosons, where they acquire mass terms through the breaking of global symmetry necessarily imposed on the model. The determination of the masses are, hence, quite important to test the model.

We have performed Monte Carlo simulations in order to estimate measurement accuracy of the masses of the heavy gauge bosons at ILC. At ILC with $\sqrt{s} = 500$ GeV, it is possible to produce A_{H} and Z_{H} bosons. Here, we can observe the excess by $A_{\text{H}} Z_{\text{H}}$ events in the

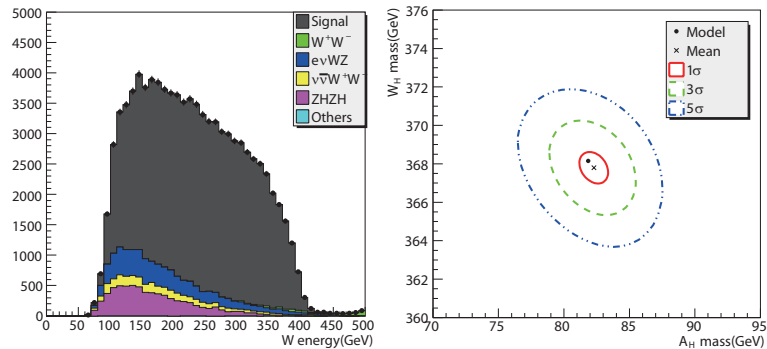


Figure 4: (a) The energy distribution of the reconstructed W bosons with remaining backgrounds after the selection cuts. (b) Probability contours corresponding to 1-, 3-, and 5- σ deviations in the A_H and W_H mass-plane.

Higgs energy distribution with the statistical significance of 3.7-sigma. Furthermore, the masses of these bosons can be determined with accuracies of 16.2% for A_H and 4.3% for Z_H . Once ILC energy reaches $\sqrt{s} = 1$ TeV, the process $e^+e^- \rightarrow W_H^+W_H^-$ opens. Since the cross section of the process is large, the masses of W_H and A_H can be determined as accurately as 1.3% and 0.2%, respectively. Then, the vacuum expectation value, f , can be determined with accuracy of 4.3% at $\sqrt{s} = 500$ GeV and 0.2% at 1 TeV.

6 Acknowledgments

The authors would like to thank all the members of the ILC physics subgroup [16] for useful discussions. This study is supported in part by the Creative Scientific Research Grant No. 18GS0202 of the Japan Society for Promotion of Science, and Dean's Grant for Exploratory Research in Graduate School of Science of Tohoku University.

References

- [1] N. Arkani-Hamed, A. G. Cohen and H. Georgi, Phys. Lett. B **513** (2001) 232;
- [2] N. Arkani-Hamed, A. G. Cohen, E. Katz and A. E. Nelson, JHEP **0207** (2002) 034.
- [3] H. C. Cheng and I. Low, JHEP **0309** (2003) 051.
- [4] H. C. Cheng and I. Low, JHEP **0408** (2004) 061.
- [5] I. Low, JHEP **0410** (2004) 067.
- [6] E. Asakawa, Phys. Rev. D **79**, 075013, (2009).
- [7] E. Komatsu *et al.* [WMAP Collaboration], arXiv:0803.0547 [astro-ph].
- [8] J. Hubisz and P. Meade, Phys. Rev. D **71** (2005) 035016, (For the correct parameter region consistent with the WMAP observation, see the figure in the revised version, hep-ph/0411264v3).
- [9] M. Asano, S. Matsumoto, N. Okada and Y. Okada, Phys. Rev. D **75** (2007) 063506;
- [10] <http://madgraph.hep.uiuc.edu/>.
- [11] <http://acfahep.kek.jp/subg/sim/softs.html>.
- [12] H. Murayama, I. Watanabe, K. Hagiwara, KEK-91-11, (1992) 184.

- [13] T. Sjöstrand, *Comp. Phys. Comm.* **82** (1994) 74.
- [14] <http://wasm.home.cern.ch/wasm/goodies.html>.
- [15] GLD Detector Outline Document, arXiv:physics/0607154.
- [16] <http://www-jlc.kek.jp/subg/physics/ilcphys/>.